

Supplementary Information for “**Photoresponse enhancement in a cavity-antenna-coupled graphene terahertz detector**”

Jie Deng,^{a,b} Jing Zhou,^{*a,b} Xu Dai^{a,b}, Yonghao Bu^{a,b}, Zhifeng Li^{a,b}, and Xiaoshuang Chen^{*a,b}

a. State Key Laboratory of Infrared Physics, Shanghai Institute of Technical Physics, Chinese

Academy of Sciences, Shanghai 200083, China

b. University of Chinese Academy of Sciences, 19 Yuquan Road, Beijing, 100049, China

Note 1. The influence of the SiO₂/Si substrate on the cavity-antenna-coupled graphene terahertz detector

The cavity-antenna-coupled graphene terahertz detector is supported by a SiO₂ (300 nm)/Si substrate. The influence of this substrate on the performance of the detector is investigated by simulation. As shown in Fig. S1 (a), when the thickness of the SiO₂ layer varies from 250 to 500 nm, the graphene absorptance remains high. Since the thickness of the SiO₂ layer is much smaller than the wavelength (1.040 mm) of the THz radiation, there is little effect of the SiO₂ layer on the cavity resonance and the graphene absorptance.

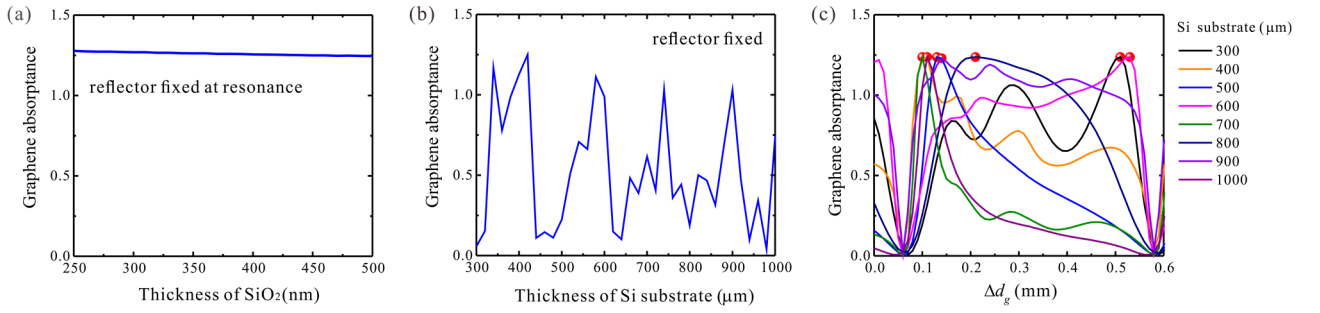


Figure S1 (a) Simulated graphene absorptance as a function of the SiO₂ layer thickness. The thickness of the Si substrate is 500 μm and the reflector is 1.63 mm away from the graphene. (b) Simulated graphene absorptance as a function of the thickness of Si silicon substrate. The thickness of the SiO₂ layer is 300 nm and the reflector is 2 mm away from the graphene. (c) Simulated d_g dependent graphene absorptance curves at different thicknesses of the Si substrate. The thickness of the SiO₂ layer is 300 nm.

The Si substrate is chosen to be highly resistive so that it is transparent to the THz wave. This substrate with a typical thickness of 500 μm contributes to the interference of the THz wave in the detector. As shown in Fig. S1 (b), the graphene absorptance is severely influenced by the thickness of the Si substrate (d_{sub}) when the reflector is fixed at the same position (2 mm away from the graphene). According to Eq. 1 and Fig. 3 in the main text, the Si substrate constitutes a part of the transmission line, thus affecting the phase accumulation. Therefore, as d_{sub} varies from 300 μm to 1000 μm , the THz wave in the cavity-antenna-coupled graphene detector experiences periodically alternating constructive and destructive interference, leading to the oscillating graphene absorptance in Fig. S1 (b). Since the phase accumulation change due to the variation in d_{sub} can be compensated by adjusting the distance between the reflector and the graphene (d_g), a constructive interference

condition can always be achieved at different d_{sub} values. Fig. S1 (c) exhibits the d_g dependent graphene absorptance curves at eight different d_{sub} values from 300 to 1000 μm . The red spheres mark the constructive interference condition at each d_{sub} value. In each curve, the graphene absorptance reaches a maximum under the constructive interference condition.

Note 2. The FET characterisation of the graphene flake

The Si substrate of the cavity-antenna-coupled graphene THz detector is made of high-resistivity Si, so it cannot be used as a gate for the graphene flake. To realize the electrostatic gating, we fabricated a new device with an extra metal back gate and a hBN insulating spacer. Fig. S3 (a) shows the optical microscopic image of the gate-tunable device, the scale bar is 10 μm . During the fabrication, the source, drain, and gate electrodes are made at first. Then, the hBN and graphene flakes are transferred to the channel region in sequence. The hBN flake covers the gate electrode in the middle of the channel region, insulating the graphene from the gate electrode. The channel is 4 μm and the width of the gate electrode is 1 μm . The graphene, hBN, and gate electrode are marked by white, blue, and yellow dash frames, respectively.

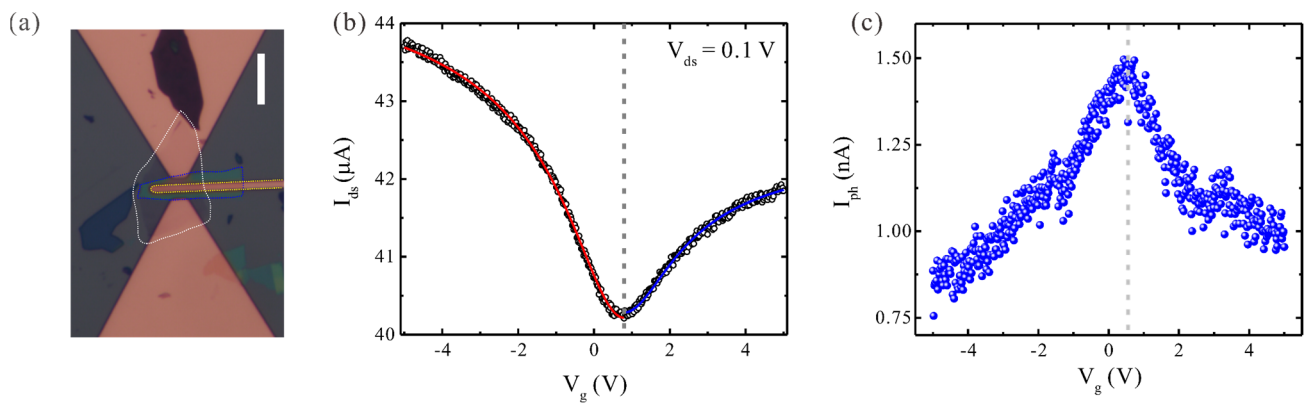


Figure S2 (a) Optical microscopic image of the gate-tunable device. The scale bar is 10 μm . The graphene, hBN, and gate electrode are by white, blue, and yellow dash frames, respectively. (b) Transfer characteristics of the graphene flake. (c) Gate-dependent photocurrent under $357 \mu\text{W}/\text{cm}^2$ illumination.

The FET characterization is measured at the $V_{ds} = 0.1 \text{ V}$ with the gating voltage (V_g) sweeping from -5 V to $+5 \text{ V}$. As shown in Fig. S2 (b), the mobility (μ), the gate voltage of the Dirac point

(V_{dirac}), and the unit capacitance of hBN (C_g) are obtained by fitting the transfer characteristics with the following equation¹:

$$R = R_{contact} + \frac{L/W}{e\mu\sqrt{n_0^2 + (C_g |V_g - V_{dirac}|)^2}}. \quad (R1)$$

$R_{contact}$ is the contact resistance, L and W are the length and width of the channel respectively, e is the element charge, and n_0 is the residual charge density. The unit capacitance of hBN is expressed by $C_g = \epsilon_0 \epsilon_{hBN} / t_{hBN}$, where ϵ_0 is the vacuum permittivity, $\epsilon_{hBN} = 3.76$ is the relative dielectric permittivity of hBN², and t_{hBN} is the thickness of the hBN flake. According to the fitting result, the thickness of hBN is about 8~10 nm, which is consistence with the color in the optical microscopic image empirically. The fitted mobility μ for holes and electrons are 1400 and 2181 $\text{cm}^2/(\text{V}\cdot\text{s})$, respectively. The Fermi level of the as-exfoliated graphene is about 150 meV below the Dirac point, and V_{dirac} is around 0.7 V. Fig. S2 (c) shows the gate-dependent photocurrent, the peak photoresponse appears around $V_g = 0.5$ V, corresponding the Fermi level $E_f \sim 90$ meV. According to our analysis about impedance matching in the main text, the doping level of the graphene influences the effective surface conductivity σ_{a-gr} of the antenna-graphene hybrid structure, thus affecting the total input impedance $Z_{in,sc}$, and the light coupling efficiency. Based on the simulation with the hole mobility of 1400 $\text{cm}^2/(\text{V}\cdot\text{s})$ in the electrostatic gating experiment, the impedance matched condition occurs at $E_f = 100$ meV, very close to the maximum-photocurrent E_f (90 meV) in the experiment. Therefore, the influence of the Fermi level on the photocurrent is attributed to the variation of light coupling. When the Fermi Level is close to 90 meV, the impedance matched condition is achieved, the absorptance of the graphene is optimized, and the photocurrent reaches the maximum.

Note 3. The performance comparison between THz detectors

Some THz detectors based on low-dimensional materials are summarized in Table S1 for comparison. Among them, No.1~3 are detectors equipped with a cavity-like structure. The rest are the sub-THz detector made of diverse low-dimensional materials (No.4~8) and graphene (No.9~19). The room-temperature graphene THz detectors with similar detection frequencies as our device have

been included in Fig. 4 (a).

Table S1 A performance comparison between sub-THz detectors at a similar operation frequency

No.	Material	Responsivity (V/W)	NEP (nW/rtHz)	Enhance ment	Freq (THz)	Ref.
1	GaN HEMT	3250	0.004	2.5	0.14	[41]
2	Nb ₅ N ₆	2.25 mV	-	9	0.275	[42]
3	Nb ₅ N ₆	1.25 mV	-	4	0.285	[42]
4	BP	7.8	7	-	~0.3	[43]
5	BP	3	7	-	3.4	[44]
6	BP	0.15	40	-	~0.3	[45]
7	MoSe ₂	0.0038	3100	-	~0.3	[46]
8	BiTeSe	3	10	-	~0.3	[47]
9	Graphene	34 μ A/W	150	-	2	[48]
10	Graphene	0.1	207	-	~0.3	[49]
11	Graphene	0.25	80	-	~0.3	[50]
12	Graphene	2	3	-	0.33~0.5	[51]
13	Graphene	70	0.13	-	0.4	[52]
14	Graphene	30	0.051	-	0.33	[53]
15	Graphene	10	1	-	0.3	[54]
16	Graphene	14	0.5	-	0.6	[55]
17	Graphene	1.7	1.3	-	0.3	[56]
18	Graphene	0.5	10	-	0.36	[57]
19	Graphene	1.2 V/W (1.3mA/W)	2	-	~0.3	[58]
20	Graphene	20.4 V/W (10.2 mA/W)	0.92	15	0.288	This work

Note 4. Concerns about the practical application of the cavity-antenna-coupled graphene THz detector

The first concern about the practical application of the cavity-antenna-coupled graphene THz detector is light power collection. Since the THz beam size (~ 10 mm) is much larger than the antenna (~ 1 mm), the power received by the detector is a small portion of the total incident power, thus hindering the practical usage. We propose to add a lens in the system to focus the incident THz wave on the detector (Fig. S4 (a)). Concerning a TPX lens with a thickness of several millimeters, the transmission is higher than 95%. As shown in Fig. S4 (b), with the focused light spot size decreasing from 10 mm to 1 mm, the responsivity increases 11 times. The graphene absorptance is normalized to that at the spot size of 10 mm. The light focusing does not affect the interference of the THz wave in the detector or the impedance matching. Thus, adding a focusing lens to our detector would significantly enhance the absorption efficiency. Actually, most optical systems relying on single-pixel detectors are equipped with focusing lenses.

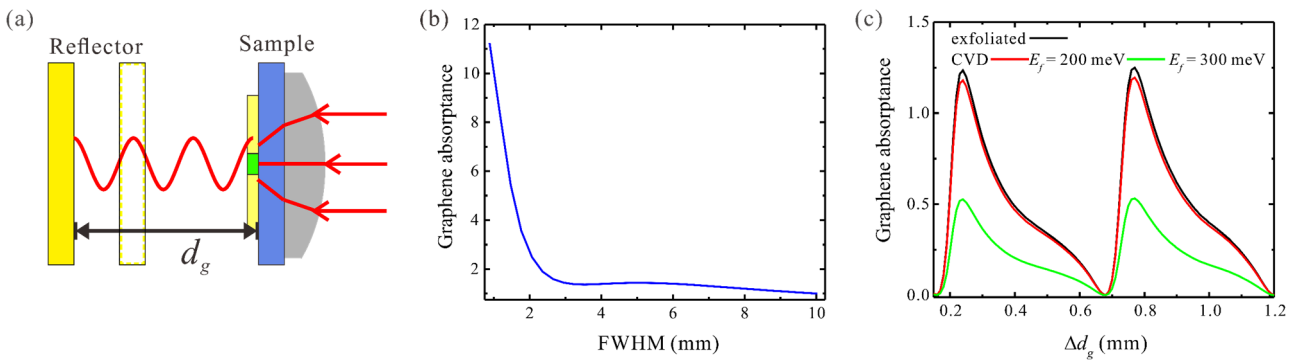


Fig. S4 (a) The schematic diagram of the detector with a focused Gaussian beam. (b) Graphene absorptance versus the focused light spot size. The graphene absorptance is normalized to that at the spot size of 10 mm. (c) Graphene absorptance curves with respect to Δd_g for cavity-antenna-coupled exfoliated and CVD graphene.

The second concern is about the scalability of the cavity-antenna-coupled graphene THz detector. As shown in Fig. S4 (c), the cavity-antenna-enhancement scheme also works for CVD-grown graphene, allowing the detectors to be wafer-scalable³. Concerning exfoliated few-layer graphene flakes, the mobility is typically within the range from 2000 to 8000 $\text{cm}^2/(\text{V}\cdot\text{s})$ ⁴⁻⁶ and the Fermi level (E_f) could

be either above or below the Dirac point within a range of ± 200 meV. In comparison, the mobility of CVD graphene, typically several hundred $\text{cm}^2/(\text{V}\cdot\text{s})$, is much lower and the Fermi energy (E_f) is several hundred meV below the Dirac point. According to the simulation result (Fig. S4 (c)), the cavity-antenna structure can also enhance the absorptance of a CVD graphene under the constructive interference condition. With the varying distance between the reflector and the antenna coupled graphene, the absorptance of the CVD graphene oscillates in the same manner as that of the exfoliated graphene. The oscillation period is 0.52 mm, half the wavelength of the THz wave. By tuning the Fermi level of the CVD graphene from 300 meV to 200 meV, the peak absorptance of graphene is enhanced from 0.5 to 1.2, close to that of the exfoliated graphene. Thus, the impedance matched condition can be reached with a CVD graphene. The cavity-antenna-enhancement scheme also works for CVD graphene.

Reference

- [1] H. Zhong, Z. Zhang, H. Xu, C. Qiu and L.-M. Peng, *AIP Advances*, 2015, **5**, 057136.
- [2] Laturia, M. L. Van de Put and W. G. Vandenberghe, *npj 2D Mater Appl*, 2018, **2**, 6.
- [3] M. Asgari, E. Riccardi, O. Balci, D. De Fazio, S. M. Shinde, J. Zhang, S. Mignuzzi, F. H. L. Koppens, A. C. Ferrari, L. Viti and M. S. Vitiello, *ACS Nano*, 2021, **15**, 17966–17976.
- [4] S. Kim, J. Nah, I. Jo, D. Shahrjerdi, L. Colombo, Z. Yao, E. Tutuc and S. K. Banerjee, *Appl. Phys. Lett.*, 2009, **94**, 062107.
- [5] V. E. Dorgan, M.-H. Bae and E. Pop, *Appl. Phys. Lett.*, 2010, **97**, 082112.
- [6] A. Venugopal, J. Chan, X. Li, C. W. Magnuson, W. P. Kirk, L. Colombo, R. S. Ruoff and E. M. Vogel, *J. Appl. Phys.*, 2011, **109**, 104511.